
Article:
Zhu, Y. and Lang, Z. (2018) Design of nonlinear systems in the frequency domain: an output frequency response function-based approach. IEEE Transactions on Control Systems Technology, 26 (4). pp. 1358-1371. ISSN 1063-6536

https://doi.org/10.1109/TCST.2017.2716379

Design of Nonlinear Systems in the Frequency Domain: An Output Frequency Response Function Based Approach

Yunpeng Zhu, Z Q Lang*

***Abstract*—In the present study, a NARX (Nonlinear Auto Regressive with eXegenous input) model of nonlinear systems, where the physical parameters of interest for the system design appear explicitly as coefficients in the model, is introduced. The model is referred to as the NARX Model with parameters of interest for Design (NARX-M-for-D). The Output Frequency Response Function (OFRF) in terms of these physical parameters is then introduced for the NARX-M-for-D, and an efficient algorithm is derived to determine the OFRF so as to facilitate the design of nonlinear systems in the frequency domain. Moreover, a general procedure for the design of the physical parameters of the NARX-M-for-D in the frequency domain is proposed, which has the potential to be applied to design a wide range of engineering systems and structures. Finally, two case studies are provided to demonstrate the new OFRF-based nonlinear system design and its significance in engineering applications.**

***Index Terms*—The OFRF; Nonlinear systems; The frequency domain; The NARX model; Engineering system design;**

I. Introduction

IN engineering practice, the design of a system is often concerned with the determination of the system parameters that can be used to achieve desired system responses under considered loadings or input excitations [1-3]. The frequency domain design of linear systems [4-6] based on the traditional concept of Frequency Response Function (FRF) has been widely applied in engineering system designs such as, e.g., the design of the dynamic properties of vibration absorbers [7], vehicle suspensions [8], and aero engine blades [9].

In practice, many systems cannot be simply described by a linear model [10]. In this case, nonlinear system analysis and design methods in either the time or the frequency domain have to be applied to study these systems. Compared with the time domain methods such as, e.g., the harmonic balance method and the multi-scale method [11], etc., the nonlinear system analysis in the frequency domain can deal with a general class of nonlinear systems rather than the systems with a specific model description [12, 13].

This analysis is achieved by using the well-known Generalized Frequency Response Functions (GFRFs) [14]. However, in spite of providing a general representation for a wide glass of nonlinear systems in the frequency domain, the GFRFs are a series of multi-dimensional functions which are often difficult to measure, display and interpret in practice. To address this issue, many new concepts such as Nonlinear Output Frequency Response Function (NOFRF) [15], Output Frequency Response Function (OFRF) [16], and Higher Order Sinusoidal Input Describing Functions (HOSIDF) [17] have been proposed. The OFRF reveals an analytical relationship between the output frequency response of nonlinear systems and the parameters which define the system nonlinearities and can be used to facilitate both the analysis and design of nonlinear systems in the frequency domain [18-19]. The HOSIDF can be considered as a special case of the OFRF [20].

Since the introduction of the OFRF in 2007 [16], many studies on the application of this concept to the nonlinear system analysis and design have been conducted. For example, Peng and Lang [21] have derived a recursive algorithm to determine the structure of the OFRF for the system described by a nonlinear differential equation model. More recently, the OFRF based approach has been applied in the analysis and design of nonlinear vibration isolators [22-24]. For example, by using the OFRF, Lang et al [22] and Peng et al [23] have rigorously proved significant beneficial effects of nonlinear damping on vibration isolation systems. Recently, Lv and Yao [24] have applied the OFRF to study the influence of damping coefficients on both the force and displacement transmissibility, showing that the nonlinear isolators can perform better than linear isolators over certain frequency ranges.

The previous studies have shown that the OFRF-based nonlinear system analysis and design have advantages and potential to solve many engineering problems. However, almost all currently available results require that a nonlinear differential equation-based physical model of the system is available in which the physical parameters that can be used for the system analysis and design are the coefficients in the differential equation model. In most cases of engineering designs, such as, e.g., vibration isolators made of viscoelastic and composite materials [25] and bladed disks of aero-engines [26], it is difficult or impossible to find such a physical model for the systems. But, it is possible to find, via a nonlinear system identification approach, a data driven NARX model representing the relationship between the input excitation and corresponding system response [27]. In addition, as demonstrated by our previous work [28], it is also possible to

This work was partly supported by the UK EPSRC and Royal Society. Yunpeng Zhu would like to acknowledge the support of Engineering Faculty Scholarship for his PhD study at Sheffield on this subject.

Yunpeng Zhu and Z. Q. Lang are with the Department of Automatic Control and Systems Engineering, The University of Sheffield, Mappin Street, Sheffield, S1 3JD, U.K. (Z Q Lang is the corresponding author; e-mail: z.lang@sheffield.ac.uk).

identify a NARX model such that the physically meaningful parameters appear explicitly as coefficients in the model. A general representation of such a NARX model is, in the present study, referred to as the NARX Model with parameters of interest for Design (NARX-M-for-D). The advantages of the OFRF in nonlinear system analysis and design as demonstrated in previous studies imply that there is a need to develop an OFRF based-approach for the NARX-M-for-D.

In the present study, the OFRF of the NARX-M-for-D in terms of the design parameters is defined. The NARX-M-for-D is a novel and general model of nonlinear systems which can be directly determined from data and used to represent complex engineering systems for the purpose of system analyses and designs. A recursive algorithm for the determination of the structure of the OFRF for a class of nonlinear systems described by a NARX-M-for-D is derived, which can directly produce an OFRF representation of the system output frequency responses without involving any complicated mathematical derivations/operations. Then, a general OFRF-based approach to the frequency domain design of nonlinear systems described by the NARX-M-for-D is proposed, which allows a systematic OFRF-based design that, for the first time, can take the effect of both the system linear and nonlinear characteristics on the design into account. The new method is an extension of the original OFRF based method to a much more general case where the OFRF for a NARX-M-for-D has to be derived and design parameters of concern can affect both linear and nonlinear characteristics of the system. Case studies are used to demonstrate the effectiveness of the proposed new design approach, showing a promising application of the OFRF based design that is expected to be able to systematically address the design problems of a wide class of engineering systems.

The paper is organized as follows. Section II introduces the NARX-M-for-D and defines the model's OFRF in terms of the system parameters of interest for design. Section III is concerned with the determination of the OFRF for a class of nonlinear systems described by the NARX-M-for-D, where an effective recursive algorithm is derived for the determination the OFRF representation of the system output frequency responses. In Section IV, a general OFRF based approach for the frequency domain design of nonlinear systems is proposed. Then, two case studies with regard to the design of the output frequency response of a nonlinear oscillator and the force transmissibility of a nonlinear vibration isolator, respectively, are presented in Section V. Finally, conclusions are given in Section VI.

II. The NARX Model with Parameters of Interest for Design and Its OFRF Representation

A. The NARX Model with parameters of interest for Design (NARX-M-for -D)

1) The concept of the NARX-M-for-D

The traditional NARX model of Single Input Single Output (SISO) nonlinear systems can be described as [29]:

$$\begin{aligned} y(t) &= f\left(y(t-1),\ldots,y(t-n_y),u(t-1),\ldots,u(t-n_u)\right) \\ &= \sum_{m=1}^{M}\sum_{p=0}^{m}\sum_{k_1,\,k_{p+q}=1}^{K}\left[c_{p,q}(k_1,k_2,\cdots,k_{p+q})\prod_{i=1}^{p}y(t-k_i)\prod_{i=p+1}^{p+q}u(t-k_i)\right] \end{aligned} \quad (1)$$

where $y(.)$ and $u(.)$ are the outputs and inputs of the system; M and K are integers, $p+q=m$ and $\sum_{k_1,k_{p+q}}^{K}=\sum_{k_1}^{K}\cdots\sum_{k_{p+q}}^{K}$; n_y and n_u are the maximum time delay of the system for $y(.)$ and $u(.)$, respectively; $f(.)$ is a nonlinear function representing the dynamic relationship between the system input and output which has, in model (1), been approximated by a polynomial function of the delayed system input and output.

In practice, the NARX model (1) can be determined by using a nonlinear system identification method from the input and output data of a system. However, the values of the coefficients $c_{p,q}(.)$ in model (1) generally have no direct physical meanings. Because of this, in most cases, the NARX model (1) is used for evaluating the system output responses to different inputs [30]. It is generally difficult to directly use the model to analyse the effects of system physical characteristics on the system behaviours so as to achieve the objectives of system designs. In order to overcome this problem, a new NARX model known as the NARX-M-for-D is introduced as follows.

The NARX-M-for-D is a NARX model where the physical parameters of interest for the system design appear explicitly as model coefficients. A general form of the single input single output NARX-M-for-D of nonlinear systems can be given as:

$$y(t)=f\left(\begin{matrix}y(t-1),\ldots,y(t-n_y),u(t),u(t-1),\ldots,\\ u(t-n_u),\boldsymbol{\theta}(\boldsymbol{\xi})\end{matrix}\right) \quad (2)$$

where $\boldsymbol{\theta}(\boldsymbol{\xi})$ is a vector representing a set of functions of the parameter vector $\boldsymbol{\xi}=[\xi_1,\ldots,\xi_S]$, where $\xi_1,\ldots,\xi_S$ are the physical parameters of interest for the system design, and S is the number of these design parameters.

Considering $f(.)$ can be approximated by a polynomial function of the delayed system input and output as in model (1), the NARX-M-for-D can further be expressed as:

$$\sum_{m=1}^{M}\sum_{p=1}^{m}\sum_{k_1,\,k_{p+q}=0}^{K}\left[\theta_{p,q}^{(k_1,k_2,\cdots,k_{p+q})}(\boldsymbol{\xi})\prod_{i=1}^{p}y(t-k_i)\prod_{i=p+1}^{p+q}u(t-k_i)\right]=0 \quad (3)$$

where $\theta_{p,q}^{(k_1,\cdots,k_{p+q})}(\boldsymbol{\xi})\in\boldsymbol{\theta}(\boldsymbol{\xi})$ with $p+q=m$ represents the coefficients of the NARX-M-for-D (3).

2) An example of the NARX-M-for-D

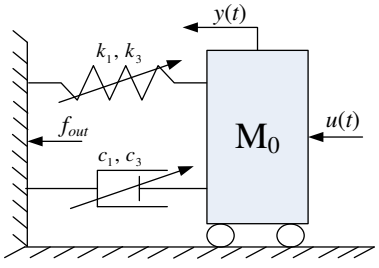

Fig.1 A nonlinear oscillator

In order to demonstrate the practical relevance of the NARX-M-for-D (3), consider a nonlinear oscillator system as

shown in Fig.1, where $M_0 = 1\,\text{kg}$, k_1, k_3, c_1 and c_3 are the oscillator parameters to be designed to achieve a desired vibration isolation performance. $u(t)$ and $y(t)$ are the input and output of the system, respectively.

The differential equation model of the system in Fig.1 is:

$$\ddot{y}(t)+c_1\dot{y}(t)+k_1y(t)+k_3y(t)^3+c_3\dot{y}(t)^3=u(t) \tag{4}$$

Considering that the first and the second derivatives in (4) can be approximated by:

$$\dot{y}(t)=\frac{y(t)-y(t-1)}{\Delta t},\ \ddot{y}(t)=\frac{y(t+1)-2y(t)+y(t-1)}{\Delta t^2} \tag{5}$$

respectively, where Δt is the sampling period, substituting (5) into (4) with $1/\Delta t = 512\,\text{Hz}$ yields a NARX-M-for-D of the system as:

$$\begin{aligned}&\theta_{0,1}^{(1)}(\boldsymbol{\xi})u(t-1)+\theta_{1,0}^{(1)}(\boldsymbol{\xi})y(t-1)+\theta_{1,0}^{(2)}(\boldsymbol{\xi})y(t-2)+\\&\theta_{3,0}^{(1,1,1)}(\boldsymbol{\xi})y^3(t-1)+\theta_{3,0}^{(1,1,2)}(\boldsymbol{\xi})y^2(t-1)y(t-2)+\\&\theta_{3,0}^{(1,2,2)}(\boldsymbol{\xi})y(t-1)y^2(t-2)+\theta_{3,0}^{(2,2,2)}(\boldsymbol{\xi})y^3(t-2)+\\&\theta_{1,0}^{(0)}(\boldsymbol{\xi})y(t)=0\end{aligned} \tag{6}$$

Eq. (6) is a specific case of the general NARX-M-for-D (3) with $\boldsymbol{\xi}=[k_1, c_1, k_3, c_3]$ and coefficients $\theta_{0,1}^{(1)}(\boldsymbol{\xi}), \theta_{1,0}^{(1)}(\boldsymbol{\xi})$, etc. given in Appendix A.1

The design of the parameters k_1, k_3, c_1 and c_1 of the nonlinear system in Fig.1 can therefore be transformed to the design of the same parameters but for the NARX-M-for-D (6).

It is worth pointing out that in order to obtain an effective discretized model, the sampling frequency $f_s = 1/\Delta t$ is required to be large enough to cover all system behaviors of interest to ensure the discretized model can sufficiently represent the original nonlinear system.

B. The OFRF of the NARX-M-for-D

The OFRF of nonlinear systems is determined based on a nonlinear differential equation model [16], where a polynomial relationship between the system output frequency response and system parameters which defines the system nonlinearities is derived. In this relationship, the coefficients of the polynomial are dependent on the system linear characteristic parameters, and the order of the polynomial is determined by the highest order in the system's Volterra series representation.

For the NARX-M-for-D (3), the OFRF concept can be introduced as described in Proposition 1 below.

Proposition 1. *Assume* $\theta_{p,q}^{(k_1,\cdots,k_{p+q})}(\boldsymbol{\xi})\in\boldsymbol{\theta}(\boldsymbol{\xi})$ *can be represented by a polynomial function of the system design parameters* $\xi_1,\ldots,\xi_S$ *up to the* n_ξ *th order such that*

$$\theta_{p,q}^{(k_1,\cdots,k_{p+q})}(\boldsymbol{\xi})=\sum_{(r_1,\cdots,r_S)\in\boldsymbol{R}_S}\beta_{(r_1,\cdots,r_S)}\xi_1^{r_1}\xi_2^{r_2}\cdots\xi_S^{r_S} \tag{7}$$

where $\boldsymbol{R}_S$ *is a set of* S *-dimensional nonnegative integer vectors which contains the exponents of* $\xi_1^{r_1}\xi_2^{r_2}\cdots\xi_S^{r_S}$, *and* $r_1,\cdots,r_S\le n_\xi$, $\beta_{(r_1,\cdots,r_S)}$ *are constants.*

The output frequency response $Y(\mathrm{j}\omega)$ *of the NARX-M-for-D can be written into a poynomial function of* $\boldsymbol{\xi}=[\xi_1,\ldots,\xi_S]$ *as*

$$Y(\mathrm{j}\omega)=\sum_{(j_1,\cdots,j_S)\in\boldsymbol{J}}\lambda_{(j_1,\cdots,j_S)}(\mathrm{j}\omega)\xi_1^{j_1}\xi_2^{j_2}\cdots\xi_S^{j_S} \tag{8}$$

where $\lambda_{(j_1,\cdots,j_S)}(\mathrm{j}\omega)$ *are the functions of frequency variable* ω *and are dependent on* $\theta_{1,0}^{(k_1)}(\boldsymbol{\xi})$ *and* $\theta_{0,1}^{(k_1)}(\boldsymbol{\xi})$ *which are the linear characteristic parameters of system (3).* $\boldsymbol{J}$ *denotes the integer vectors. (8) is the OFRF of the NARX-M-for-D (3).*

Proof of Proposition 1. Omitted due to the limited space.

Remark 1: In the case of the NARX-M-for-D (6) of system (4), the parameters of interest for the system design are k_3 and c_3, and the OFRF can be obtained as:

$$\begin{aligned}Y(\mathrm{j}\omega)=&\lambda_{(0,0)}(\mathrm{j}\omega)+\lambda_{(1,0)}(\mathrm{j}\omega)k_3+\lambda_{(0,1)}(\mathrm{j}\omega)c_3+\\&\lambda_{(2,0)}(\mathrm{j}\omega)k_3^2+\lambda_{(1,1)}(\mathrm{j}\omega)k_3c_3+\lambda_{(0,2)}(\mathrm{j}\omega)c_3^2+\cdots\end{aligned} \tag{9}$$

where $\lambda_{(j_1,j_2)}(\mathrm{j}\omega)$, $j_1, j_2 = 0,1,\ldots$ are the functions of ω and dependent on the system linear parameters c_1 and k_1. Also, it can be shown that the OFRF of the NARX-M- for-D (6) given by (9) is the same as the OFRF that can be determined from the differential equation model (4) of the system. This implies that, instead of using a physically meaningful differential equation model, the NARX-M-for-D of a nonlinear system can equally be used to perform the OFRF-based system analysis and design.

Remark 2: It is worth pointing out that in most cases the differential equation model of complex nonlinear systems is difficult even impossible to be obtained. In these cases, the NARX-M-for-D of the system needs to be determined by using a nonlinear system identification approach which involves procedures to determine both model structure and coefficients as well as deal with noise and model mismatch etc. problems as demonstrated in our previous work in [28] and other relevant works [27, 30].

Remark 3: Given the order of system nonlinearity to be taken into account, the OFRF of the NARX-M-for-D is a unique polynomial form representation for the system's output spectrum [16]. The increase of the system design parameters may increase the complexity of the OFRF. But, different from numerical approximation or curve fitting, there is no overfitting issue because of the OFRF's uniqueness.

In order to use the OFRF of a NARX-M-for-D to perform the system analysis and design, it is very important that the "structure" and "coefficients" of the OFRF representation have to be determined. The OFRF "structure" basically refers to the monomials that need to be included in the OFRF representation, whilst the "coefficients" are the value of $\lambda_{(j_1,\cdots,j_S)}(\mathrm{j}\omega)$ associated with each monomial in the OFRF. In next section, these issues will be addressed for a more general NARX-M- for-D where the NARX-M-for-D (2) or (3) is a special case.

III. Determination of the OFRFs Described by a More General NARX-M-for-D

A. A more general NARX-M-for-D

Consider the nonlinear systems which can be described by the following more general NARX-M-for-D and are stable at zero equilibrium:

$$\sum_{m=1}^{M_1}\sum_{p=0}^{m}\sum_{k_1,\,k_{p+q}=0}^{K}\left[\bar{\theta}_{p,q}^{(k_1,\cdots,k_{p+q})}(\boldsymbol{\xi})\prod_{i=1}^{p}x(t-k_i)\prod_{i=p+1}^{p+q}u(t-k_i)\right]=0 \tag{10a}$$

$$\sum_{m=1}^{M_2}\sum_{p=0}^{m}\sum_{k_1,\,k_{p+q}=0}^{K}\left[\tilde{\theta}_{p,q}^{(k_1,\cdots,k_{p+q})}(\boldsymbol{\xi})\prod_{i=1}^{p}x(t-k_i)\prod_{i=p+1}^{p+q}u(t-k_i)\right]-y(t)=0 \tag{10b}$$

where $p+q=m$, M_1, M_2 are positive integers. $u(.)$ is the input and $x(.)$, $y(.)$ are two outputs of the system.

Basically, the NARX-M-for-D (10) represents a single input double output nonlinear system. (10a) is essentially the same as the NARX-M-for-D (2) or (3), whilst (10b) describes how a second system output $y(t)$ is determined by the system input $u(t)$ and the first output $x(t)$.

If the model coefficients are constants, system (10) is basically the one input two output NARX model considered in Jing et al [31]. The GFRFs of system (10) with respect to system output $x(t)$ can be determined recursively from the parameters of the system time domain model (10a) as [29]:

$$\begin{aligned}&\left[1-\sum_{k_1=0}^{K}\bar{\theta}_{1,0}^{(k_1)}(\boldsymbol{\xi})\exp\left(-\mathrm{j}\left(\omega_1+\cdots+\omega_n\right)k_1\Delta t\right)\right]H_n^x(\omega_1,\cdots,\omega_n)\\&=\sum_{k_1,\,k_n=0}^{K}\bar{\theta}_{0,n}^{(k_1,\cdots,k_n)}(\boldsymbol{\xi})\exp\left(-\mathrm{j}\left(\omega_1k_1+\cdots+\omega_nk_n\right)\Delta t\right)\\&\quad+\sum_{q=1}^{n-1}\sum_{p=1}^{n-q}\sum_{k_1,\,k_n=0}^{K}\left[\bar{\theta}_{p,q}^{(k_1,\cdots,k_{p+q})}(\boldsymbol{\xi})H_{n-q,p}(\omega_1,\cdots,\omega_{n-q})\right.\\&\quad\left.\times\exp\left(\mathrm{j}\left(\omega_{n-q+1}k_{p+1}+\cdots+\omega_nk_{p+q}\right)\Delta t\right)\right]\\&\quad+\sum_{p=2}^{n}\sum_{k_1,\,k_p=0}^{K}\left[\bar{\theta}_{p,0}^{(k_1,\cdots,k_p)}(\boldsymbol{\xi})H_{n,p}(\omega_1,\cdots,\omega_n)\right]\end{aligned} \tag{11a}$$

with

$$\begin{cases}H_{n,p}(\omega_1,\cdots,\omega_n)=\displaystyle\sum_{i=1}^{n-(p-1)}H_i^x(\omega_1,\cdots,\omega_i)H_{n-i,p-1}(\omega_{i+1},\cdots,\omega_n)\\\qquad\qquad\times\exp\left(-\mathrm{j}\left(\sum_{l=1}^{i}\omega_l\right)k_p\Delta t\right)\\H_{n,1}(\omega_1,\cdots,\omega_n)=H_n^x(\omega_1,\cdots,\omega_n)\exp\left(-\mathrm{j}\left(\omega_1+\cdots+\omega_n\right)k_1\Delta t\right)\end{cases}$$

where Δt is the sampling time of the discrete time system, $H_n^x(\omega_1,\cdots,\omega_n), n=1,2,\ldots$ represents the n th order GFRFs of system (10) with respect to the output $x(t)$, and $\omega_i, i=1,2,\ldots$ are physical frequency variables.

Similarly, it can be shown that the GFRFs of system (10) with respect to system output $y(t)$ can be determined from the parameters of the system time domain model as

$$\begin{aligned}H_n^y(\omega_1,\cdots,\omega_n)&=\sum_{k_1,\,k_n=0}^{K}\tilde{\theta}_{0,n}^{(k_1,\cdots,k_n)}(\boldsymbol{\xi})\exp\left(-\mathrm{j}\left(\omega_1k_1+\cdots+\omega_nk_n\right)\Delta t\right)\\&\quad+\sum_{q=1}^{n-1}\sum_{p=1}^{n-q}\sum_{k_1,\,k_n=0}^{K}\left[\tilde{\theta}_{p,q}^{(k_1,\cdots,k_{p+q})}(\boldsymbol{\xi})H_{n-q,p}(\omega_1,\cdots,\omega_{n-q})\right.\\&\quad\left.\times\exp\left(\mathrm{j}\left(\omega_{n-q+1}k_{p+1}+\cdots+\omega_nk_{p+q}\right)\Delta t\right)\right]\\&\quad+\sum_{p=1}^{n}\sum_{k_1,\,k_p=0}^{K}\left[\tilde{\theta}_{p,0}^{(k_1,\cdots,k_p)}(\boldsymbol{\xi})H_{n,p}(\omega_1,\cdots,\omega_n)\right]\end{aligned} \tag{11b}$$

where $H_n^y(\omega_1,\cdots,\omega_n), n=1,2,\ldots$ represents the n th order GFRFs with respect to the system output $y(t)$.

Note that $H_{n,p}(.)$ in (11b) is the same as that in (11a) as the nonlinearities in (10b) is not related to $y(t)$. Moreover, from [16], it is known that the output frequency responses of system (10) can be represented as

$$\begin{aligned}X(\mathrm{j}\omega)&=\sum_{n=1}^{N}X_n(\mathrm{j}\omega)\\&=\sum_{n=1}^{N}\frac{1}{\sqrt{n}(2\pi)^{n-1}}\int_{\omega_1+\cdots+\omega_n=\omega}H_n^x(\omega_1,\ldots,\omega_n)\prod_{i=1}^{n}U(\mathrm{j}\omega_i)\mathrm{d}\sigma_\omega\end{aligned} \tag{12a}$$

$$\begin{aligned}Y(\mathrm{j}\omega)&=\sum_{n=1}^{N}Y_n(\mathrm{j}\omega)\\&=\sum_{n=1}^{N}\frac{1}{\sqrt{n}(2\pi)^{n-1}}\int_{\omega_1+\cdots+\omega_n=\omega}H_n^y(\omega_1,\ldots,\omega_n)\prod_{i=1}^{n}U(\mathrm{j}\omega_i)\mathrm{d}\sigma_\omega\end{aligned} \tag{12b}$$

where N is the maximum order of the system nonlinearity in the system's Volterra series representation.

From Eqs. (11) and (12), an effective algorithm can be derived to determine the OFRF representation of the spectra of the outputs $x(t)$ and $y(t)$ of system (10).

B. Determination of the OFRF structure

Assuming that the coefficients of system (10) can be expressed as a polynomial function of the system design parameters like Eq. (7), these coefficients can be written into a matrix form as:

$$\begin{cases}\bar{\theta}_{p,q}^{(k_1,\cdots,k_{p+q})}(\boldsymbol{\xi})=\bar{\boldsymbol{\xi}}_{p,q}^{(k_1,\cdots,k_{p+q})}\bar{\boldsymbol{\beta}}_{p,q}^{(k_1,\cdots,k_{p+q})}\\\tilde{\theta}_{p,q}^{(k_1,\cdots,k_{p+q})}(\boldsymbol{\xi})=\tilde{\boldsymbol{\xi}}_{p,q}^{(k_1,\cdots,k_{p+q})}\tilde{\boldsymbol{\beta}}_{p,q}^{(k_1,\cdots,k_{p+q})}\end{cases} \tag{13}$$

where $p+q>0$, $\bar{\boldsymbol{\xi}}_{p,q}^{(k_1,\cdots,k_{p+q})}$ and $\tilde{\boldsymbol{\xi}}_{p,q}^{(k_1,\cdots,k_{p+q})}$ are two vectors composed of the monomials of the form of $\xi_1^{\bar{r}_1}\xi_2^{\bar{r}_2}\cdots\xi_S^{\bar{r}_S}$ and $\xi_1^{\tilde{r}_1}\xi_2^{\tilde{r}_2}\cdots\xi_S^{\tilde{r}_S}$, respectively. $\bar{\boldsymbol{\beta}}_{p,q}^{(k_1,\cdots,k_{p+q})}$ and $\tilde{\boldsymbol{\beta}}_{p,q}^{(k_1,\cdots,k_{p+q})}$ are the two constant vectors of a corresponding dimension.

Based on the results in Section III-A, a recursive algorithm for determining the structure of the OFRFs of system (10) can be derived are described in the following propositions.

Proposition 2. *For system (10), given $H_1^x(\mathrm{j}\omega)$, $H_1^y(\mathrm{j}\omega)$ and the input spectrum $U(\mathrm{j}\omega)$, the n th order output spectra of nonlinear system (10) can be expressed as:*

$$X_n(\mathrm{j}\omega)=\bar{\boldsymbol{\Xi}}_n\boldsymbol{X}_n(\mathrm{j}\omega)\ \text{ and }\ Y_n(\mathrm{j}\omega)=\tilde{\boldsymbol{\Xi}}_n\boldsymbol{Y}_n(\mathrm{j}\omega) \tag{14}$$

and the output spectra of system (10) can be expressed as:

$$X(\mathrm{j}\omega)=\sum_{n=1}^{N}\bar{\boldsymbol{\Xi}}_n\boldsymbol{X}_n(\mathrm{j}\omega)\ \text{ and }\ Y(\mathrm{j}\omega)=\sum_{n=1}^{N}\tilde{\boldsymbol{\Xi}}_n\boldsymbol{Y}_n(\mathrm{j}\omega) \tag{15}$$

In Eq. (14) and Eq. (15), $\bar{\boldsymbol{\Xi}}_n$ and $\tilde{\boldsymbol{\Xi}}_n$ are the vectors whose components are the monomials of the system design parameters of interest that have contribution to the n th order nonlinear output of the system, $\boldsymbol{X}_n(\mathrm{j}\omega)$ and $\boldsymbol{Y}_n(\mathrm{j}\omega)$ are vectors with corresponding dimensions whose components are dependent only on $H_1^x(\mathrm{j}\omega)$, $H_1^y(\mathrm{j}\omega)$ and the frequency variable ω.

Proof of Proposition 2. See Appendix B.

Proposition 3. *The vectors $\bar{\boldsymbol{\Xi}}_n$ and $\tilde{\boldsymbol{\Xi}}_n$ introduced in Proposition 2 can be determined recursively using an algorithm as follows:*

$$\bar{\boldsymbol{\Xi}}_n = \left[\bigcup_{k_1,\ldots,k_n=0}^{K} \bar{\boldsymbol{\xi}}_{0,n}^{(k_1,\cdots,k_n)}\right] \cup \left[\bigcup_{q=1}^{n-1}\bigcup_{p=1}^{n-q}\bigcup_{k_1,\ldots,k_n=0}^{K}\left(\bar{\boldsymbol{\xi}}_{p,q}^{(k_1,\cdots,k_{p+q})} \otimes \bar{\boldsymbol{\Xi}}_{n-q,p}\right)\right] \cup \left[\bigcup_{p=2}^{n}\bigcup_{k_1,\ldots,k_n=0}^{K}\left(\bar{\boldsymbol{\xi}}_{p,0}^{(k_1,\cdots,k_p)} \otimes \bar{\boldsymbol{\Xi}}_{n,p}\right)\right] \tag{16a}$$

$$\tilde{\boldsymbol{\Xi}}_n = \left[\bigcup_{k_1,\ldots,k_n=0}^{K} \tilde{\boldsymbol{\xi}}_{0,n}^{(k_1,\cdots,k_n)}\right] \cup \left[\bigcup_{q=1}^{n-1}\bigcup_{p=1}^{n-q}\bigcup_{k_1,\ldots,k_n=0}^{K}\left(\tilde{\boldsymbol{\xi}}_{p,q}^{(k_1,\cdots,k_{p+q})} \otimes \bar{\boldsymbol{\Xi}}_{n-q,p}\right)\right] \cup \left[\bigcup_{p=2}^{n}\bigcup_{k_1,\ldots,k_n=0}^{K}\left(\tilde{\boldsymbol{\xi}}_{p,0}^{(k_1,\cdots,k_p)} \otimes \bar{\boldsymbol{\Xi}}_{n,p}\right)\right] \tag{16b}$$

where the symbol "$\otimes$" is the Kronecker product with

$$\bar{\boldsymbol{\Xi}}_1 = \tilde{\boldsymbol{\Xi}}_1 = [1] \tag{17}$$

$$\bar{\boldsymbol{\Xi}}_{n,p} = \bigcup_{i=1}^{n-p+1}\left(\bar{\boldsymbol{\Xi}}_i \otimes \bar{\boldsymbol{\Xi}}_{n-i,p-1}\right) \text{ and } \bar{\boldsymbol{\Xi}}_{n,1} = \bar{\boldsymbol{\Xi}}_n \tag{18}$$

Proof of Proposition 3. See Appendix C.

Proposition 3 provides an efficient algorithm for the determination of the monomials that need to be included in the OFRF representation for the output $X(\mathrm{j}\omega)$ and $Y(\mathrm{j}\omega)$ of the more general NARX-M-for-D (10). Although the OFRF structure is theoretically related to the system model and can be determined in an analytical way, Proposition 3 provides an algorithm which can readily be implemented using computer codes to automatically produce all the monomials in the OFRF.

According to Proposition 3, the OFRF of the output spectra of the NARX-M-for-D (10) can, like (8), be represented by polynomial function of the design parameters $\xi_1, \xi_2, \cdots, \xi_S$. A special case of Proposition 3 is given in Corollary 1 as follows.

Corollary 1. *In the special case where* $\tilde{\theta}_{p,q}^{(k_1,\cdots,k_{p+q})}(\boldsymbol{\xi}) = \alpha\bar{\theta}_{p,q}^{(k_1,\cdots,k_{p+q})}(\boldsymbol{\xi})$ *with* α *being a non-zero constant, the OFRF representation of the output spectra of NARX-M-for-D (10) can be described as:*

$$\begin{aligned} Y(\mathrm{j}\omega) &= \boldsymbol{Y}_1(\mathrm{j}\omega) + \tilde{\boldsymbol{\Xi}}_2\boldsymbol{Y}_2(\mathrm{j}\omega) + \cdots + \tilde{\boldsymbol{\Xi}}_N\boldsymbol{Y}_N(\mathrm{j}\omega) \\ &= \sum_{(\bar{j}_1,\ldots,\bar{j}_S)\in\bar{\boldsymbol{J}}} \tilde{\lambda}_{(\bar{j}_1,\ldots,\bar{j}_S)}(\mathrm{j}\omega)\xi_1^{\bar{j}_1}\xi_2^{\bar{j}_2}\cdots\xi_S^{\bar{j}_S} \end{aligned} \tag{20}$$

In (19) and (20), $\bar{\lambda}_{\bar{j}_1,\ldots,\bar{j}_S}(\mathrm{j}\omega)$ *and* $\tilde{\lambda}_{(\bar{j}_1,\ldots,\bar{j}_S)}(\mathrm{j}\omega)$ *are the functions of the same nature as* $\lambda_{(j_1,\ldots,j_S)}(\mathrm{j}\omega)$ *in Proposition 1, and the monomials in Eq. (19) and Eq. (20) are the same, which can be found from the components of*

$$\tilde{\boldsymbol{\Xi}} = \bar{\boldsymbol{\Xi}} = \bigcup_{n=1}^{N}\bar{\boldsymbol{\Xi}}_n \tag{21}$$

Proof of Corollary 1. See Appendix D.

C. Evaluation of the OFRF coefficients

It is known from Corollary 1, Proposition 2 that, the evaluation of the coefficients of the OFRF of the NARX-M-for-D (10) involves determining $\bar{\lambda}_{(\bar{j}_1,\ldots,\bar{j}_S)}(\mathrm{j}\omega)$ and $\tilde{\lambda}_{(\bar{j}_1,\ldots,\bar{j}_S)}(\mathrm{j}\omega)$ in (19) and (20), respectively. These coefficients are generally dependent on the frequency variable ω, the system input, as well as the system linear characteristic parameters. When all of these are fixed, these coefficients are constants and can be numerically evaluated as described in Proposition 4 below.

Proposition 4. *Assume that the coefficients* $\bar{\lambda}_{(\bar{j}_1,\ldots,\bar{j}_S)}(\mathrm{j}\omega)$ *in the OFRF (19) are independent of the system design parameters* $\xi_1, \xi_2, \cdots, \xi_S \in \boldsymbol{\xi}$. *Given the monomial vector*

$$\begin{aligned} \bar{\boldsymbol{\Xi}} &= \left[1, \bar{\boldsymbol{\Xi}}_2, \cdots, \bar{\boldsymbol{\Xi}}_N\right] = \left[\xi_1^{\bar{j}_1}\xi_2^{\bar{j}_2}\cdots\xi_S^{\bar{j}_S} \,\middle|\, (\bar{j}_1,\ldots,\bar{j}_S) \in \bar{\boldsymbol{J}}\right] \\ &\subseteq \left[\bigcup_{\bar{j}_1=0}^{m_1}\cdots\bigcup_{\bar{j}_S=0}^{m_S}\xi_1^{\bar{j}_1}\xi_2^{\bar{j}_2}\cdots\xi_S^{\bar{j}_S}\right] \end{aligned} \tag{22}$$

where m_i *is the maximum power of* $\xi_i, i = 1,\ldots,S$ *that has been determined by using Proposition 3, denote*

$$\bar{\boldsymbol{\Xi}}_{(j)} = \left[1, \bar{\boldsymbol{\Xi}}_{2,(j)}, \cdots, \bar{\boldsymbol{\Xi}}_{N,(j)}\right] = \left[\bar{\boldsymbol{\Xi}}_{(j)}(1), \cdots, \bar{\boldsymbol{\Xi}}_{(j)}(\bar{M})\right] \tag{23}$$

as the vector $\bar{\boldsymbol{\Xi}}$ *evaluated at the* j *th set of the system design parameters* $\xi_i(j), i = 1,\ldots,S$, $\bar{M}$ *as the total number of designs that have been initially tried. Then the OFRF representation of the system output spectrum under the* j *th set of initial design can be written as*

$$\begin{aligned} X_{(j)}(\mathrm{j}\omega) &= \left[\bar{\boldsymbol{\Xi}}_{(j)}(1), \cdots, \bar{\boldsymbol{\Xi}}_{(j)}(\bar{M})\right] \times \boldsymbol{\Lambda}_{\bar{M}\times 1} \\ &= \left[\bar{\boldsymbol{\Xi}}_{(j)}(1)/l_1, \cdots, \bar{\boldsymbol{\Xi}}_{(j)}(\bar{M})/l_M\right] \times \tilde{\boldsymbol{\Lambda}}_{\bar{M}\times 1} \end{aligned} \tag{24}$$

where $\boldsymbol{\Lambda}_{\bar{M}\times 1}$ *is a* $\bar{M}$ *dimensional vector whose components are the coefficients of the OFRF (19) and*

$$\boldsymbol{L} = [l_1, \ldots, l_{\bar{M}}]; l_i > 0, i = 1,\ldots,\bar{M} \tag{25}$$

is a constant vector, and

$$\tilde{\boldsymbol{\Lambda}}_{\bar{M}\times 1} = \left[l_1\boldsymbol{\Lambda}_{\bar{M}\times 1}(1), \ldots, l_{\bar{M}}\boldsymbol{\Lambda}_{\bar{M}\times 1}(\bar{M})\right]^{\mathrm{T}} \tag{26}$$

are the coefficients in the representation of (24). Moreover, the coefficients in (24) can be determined as

$$\tilde{\boldsymbol{\Lambda}}_{\bar{M}\times 1} = \left(\tilde{\boldsymbol{P}}_{\bar{N}\times\bar{M}}{}^{\mathrm{T}}\tilde{\boldsymbol{P}}_{\bar{N}\times\bar{M}}\right)^{-1}\tilde{\boldsymbol{P}}_{\bar{N}\times\bar{M}}{}^{\mathrm{T}}\bar{\boldsymbol{X}}_{\bar{N}\times 1} \tag{27}$$

where

$$\tilde{\boldsymbol{P}}_{\bar{N}\times\bar{M}} = \begin{bmatrix} \bar{\boldsymbol{\Xi}}_{(1)}(1)/l_1 & \cdots & \bar{\boldsymbol{\Xi}}_{(1)}(\bar{M})/l_{\bar{M}} \\ \vdots & \ddots & \vdots \\ \bar{\boldsymbol{\Xi}}_{(\bar{N})}(1)/l_1 & \cdots & \bar{\boldsymbol{\Xi}}_{(\bar{N})}(\bar{M})/l_{\bar{M}} \end{bmatrix}_{\bar{N}\times\bar{M}} \tag{28}$$

and

$$\bar{\boldsymbol{X}}_{\bar{N}\times 1} = \left[X_{(1)}(\mathrm{j}\omega), \ldots, X_{(\bar{N})}(\mathrm{j}\omega)\right]^{\mathrm{T}} \tag{29}$$

is a vector the components of which are the system output frequency responses under $\bar{N} \geq \bar{M}$ *different pilot designs.*

Proof of Proposition 4. Proposition 4 can be proved by using the traditional Least Square (LS) algorithm.

Remark 4: The LS algorithm is a very basic method that can be applied as shown in Proposition 4 to determine coefficients of the OFRF using the system response data generated from a number of prototype designs. The introduction of the constant vector $\boldsymbol{L}$ in (25) is to ensure the numerical stability of the LS solution (27). When $\boldsymbol{L} = [1,\ldots,1]$, (27) produces the coefficients of the OFRF (19), that is

$$\tilde{\boldsymbol{\Lambda}}_{\bar{M}\times 1} = \boldsymbol{\Lambda}_{\bar{M}\times 1} \tag{30}$$

Otherwise, the coefficient vector $\tilde{\boldsymbol{\Lambda}}_{\tilde{M}\times 1}$ evaluated from (27) is different from the coefficient vector of the original OFRF (19). This is needed in many practical cases to circumvent the problems numerically induced by significant difference between the values of different design parameters.

Remark 5: It is known from Proposition 4 that a change of the values of system design parameters is required to determine the OFRF representation of a system. As the NARX-M-for-D is established by either a nonlinear system identification or a discretization process, the algorithm in Proposition 4 can be implemented using a NARX-M-for-D based simulation Therefore, there is no need to literally change the values of the system's physical parameters.

Remark 6: In general, the maximum order N of the system nonlinearity is pre-determined. The error of a nonlinear system's OFRF representation is induced by the truncation error associated with the Nth order Volterra series representation of the system. The increase of the order N will reduce the error of the representation. In practice, up to 3-5th order system nonlinearity is often sufficient to use in an OFRF representation for the output frequency response of nonlinear systems [13, 16].

D. The OFRF based design of nonlinear systems

The OFRF provides an analytical representation of the output spectrum of nonlinear systems. When the OFRF of a NARX-M-for-D has been determined using the algorithm derived above. The problem of the system design can be described as a constrained optimization problem and formulated as follows.

Find the values of the system physical parameters of interest for the design:

$$\boldsymbol{\xi}_0 = [\xi_1, \ldots, \xi_S] \tag{31a}$$

to solve the optimization problem

$$\underset{\{\xi_1,\ldots,\xi_S\}}{\text{MIN}} \left| \sum_{(j_1,\ldots,j_S)\in \boldsymbol{J}} \lambda_{(j_1,\ldots,j_S)}(\mathrm{j}\omega)\xi_1^{j_1}\cdots\xi_S^{j_S} - Y_0(\mathrm{j}\omega) \right|; \omega \in \Omega \tag{31b}$$

under the constraint:

$$g_i(\xi_1,\cdots,\xi_S) \le 0; i = 1,\ldots,m \tag{31c}$$

In (31), Ω is the frequency range over which the design is considered, $Y_0(\mathrm{j}\omega)$ is a desired system output spectrum and $g_i(\xi_1,\cdots,\xi_S)$, $i = 1,\ldots,m$ are the functions associated with the design constraints.

The approach to the solution to the design problem (31) can be summarized in a procedure of five steps as follows.

Procedure of the OFRF based Design

1: **System modelling:** Establish a NARX-M-for-D for the nonlinear system by either discretizing an available differential equation model of the system or using a nonlinear system identification method.

2: **Identify model coefficients:**
(i) Nonlinear coefficients: Identify the NARX-N-for-D coefficients which define the system nonlinearity and find the relationship between the coefficients and system design parameters $\theta_{p,q}^{(k_1,\cdots,k_{p+q})}(\boldsymbol{\xi}) \in \boldsymbol{\theta}(\boldsymbol{\xi})$ where $p+q>1$.
(ii) Linear coefficients: Identify the coefficients of the NARX-M-for-D which define the system linear characteristics and the relationship between these coefficients and system design parameters $\theta_{1,0}^{(k_1)}(\boldsymbol{\xi})$ and $\theta_{0,1}^{(k_1)}(\boldsymbol{\xi})$

3: **Determine the design constraints:** Determine the system linear characteristic parameters $\theta_{1,0}^{(k_1)}(\boldsymbol{\xi})$ and $\theta_{0,1}^{(k_1)}(\boldsymbol{\xi})$ as required by the design for the FRF of the linear part of the system

$$H_1(\mathrm{j}\omega) = \frac{\sum_{k_1=1}^{K}\theta_{0,1}^{(k_1)}(\boldsymbol{\xi})\exp(-\mathrm{j}\omega k_1\Delta t)}{1-\sum_{k_1=1}^{K}\theta_{1,0}^{(k_1)}(\boldsymbol{\xi})\exp(-\mathrm{j}\omega k_1\Delta t)} \tag{32}$$

and establish a constraint for the design given by (31c) such that $H_1(\mathrm{j}\omega)$ is independent from the variation of the system design parameters $\xi_1,\cdots,\xi_S$.

4: **Formulation of the design problem:** Determine the OFRF of the NARX-M-for-D using the algorithm in Section III and formulate the optimization design problem (31).

5: **Optimal design:** Solve the optimization design problem (31) to find a solution to the design.

Remark 7: The specific form of the design constraint (31c) is determined by the practical requirements for the design. However, it is worth pointing out that the design constraint (31c) also has to make sure that the OFRF coefficients $\lambda_{(j_1,\ldots,j_S)}(\mathrm{j}\omega)$ are independent of the design parameters $\xi_1,\ldots,\xi_S \in \boldsymbol{\xi}$. This is required by the method used to evaluate the OFRF coefficients in Section III-C.

IV. CASE STUDIES

In this section, two case studies will be conducted to demonstrate the new OFRF-based nonlinear system design and its significance in engineering applications.

A. Case study 1

Consider the nonlinear system in Fig.1 where the outputs are displacement $y(t)$ and $f_{out}(t)$ is the force transmitted to the wall. The differential equation description of the system is given by

$$\begin{cases} u(t) = \ddot{y}(t) + c_1\dot{y}(t) + k_1 y(t) + k_3 y(t)^3 + c_3\dot{y}(t)^3 \\ f_{out}(t) = c_1\dot{y}(t) + k_1 y(t) + k_3 y(t)^3 + c_3\dot{y}(t)^3 \end{cases} \tag{33}$$

Discreting (33) using (5) and sampling frequency f_s = 512 Hz yields a specific case of the NARX-M-for-D (10) as

$$\begin{cases} \bar{\theta}_{0,1}^{(1)}(\boldsymbol{\xi})u(t-1) + \bar{\theta}_{1,0}^{(0)}(\boldsymbol{\xi})y(t) + \bar{\theta}_{1,0}^{(1)}(\boldsymbol{\xi})y(t-1) \\ \quad + \bar{\theta}_{1,0}^{(2)}(\boldsymbol{\xi})y(t-2) + \bar{\theta}_{3,0}^{(1,1,1)}(\boldsymbol{\xi})y^3(t-1) \\ \quad + \bar{\theta}_{3,0}^{(1,1,2)}(\boldsymbol{\xi})y^2(t-1)y(t-2) + \bar{\theta}_{3,0}^{(2,2,2)}(\boldsymbol{\xi})y^3(t-2) \\ \quad + \bar{\theta}_{3,0}^{(1,2,2)}(\boldsymbol{\xi})y(t-1)y^2(t-2) = 0 \\ \tilde{\theta}_{1,0}^{(1)}(\boldsymbol{\xi})y(t-1) + \tilde{\theta}_{1,0}^{(2)}(\boldsymbol{\xi})y(t-2) + \tilde{\theta}_{3,0}^{(1,1,1)}(\boldsymbol{\xi})y^3(t-1) \\ \quad + \tilde{\theta}_{3,0}^{(1,1,2)}(\boldsymbol{\xi})y^2(t-1)y(t-2) + \tilde{\theta}_{3,0}^{(1,2,2)}(\boldsymbol{\xi})y(t-1)y^2(t-2) \\ \quad + \tilde{\theta}_{3,0}^{(2,2,2)}(\boldsymbol{\xi})y^3(t-2) - f_{out}(t-1) = 0 \end{cases} \tag{34}$$

where $\boldsymbol{\xi}=[k_1, c_1, k_3, c_3]$ is the vector of design parameters, and the coefficients $\bar{\theta}_{0,1}^{(1)}(\boldsymbol{\xi}), \bar{\theta}_{1,0}^{(0)}(\boldsymbol{\xi})$, etc. in (34) are given in Appendix A.2 indicating that Corollary 1 is satisfied in this case.

Consider $N=5$. Then, according to Corollary 1 and using Proposition 3, the structure of the OFRF, i.e., the monomials that are involved in the OFRF representation of the output spectra $Y(\mathrm{j}\omega)$ and $F_{out}(\mathrm{j}\omega)$ of system (4) can be obtained as:

$$\tilde{\boldsymbol{\Xi}}=\bar{\boldsymbol{\Xi}}=\bigcup_{n=1}^{N}\bar{\boldsymbol{\Xi}}_n=\left[1, k_3, c_3, {k_3}^2, {c_3}^2, k_3c_3\right] \tag{35}$$

Therefore, the OFRF of NARX-M-for-D (34) can be represented as:

$$\begin{aligned}Y(\mathrm{j}\omega)=&\bar{\lambda}_{(0,0)}(\mathrm{j}\omega)+\bar{\lambda}_{(1,0)}(\mathrm{j}\omega)k_3+\bar{\lambda}_{(0,1)}(\mathrm{j}\omega)c_3+\\&\bar{\lambda}_{(2,0)}(\mathrm{j}\omega){k_3}^2+\bar{\lambda}_{(1,1)}(\mathrm{j}\omega)k_3c_3+\bar{\lambda}_{(0,2)}(\mathrm{j}\omega){c_3}^2\end{aligned} \tag{36a}$$

$$\begin{aligned}F_{out}(\mathrm{j}\omega)=&\tilde{\lambda}_{(0,0)}(\mathrm{j}\omega)+\tilde{\lambda}_{(1,0)}(\mathrm{j}\omega)k_3+\tilde{\lambda}_{(0,1)}(\mathrm{j}\omega)c_3+\\&\tilde{\lambda}_{(2,0)}(\mathrm{j}\omega){k_3}^2+\tilde{\lambda}_{(1,1)}(\mathrm{j}\omega)k_3c_3+\tilde{\lambda}_{(0,2)}(\mathrm{j}\omega){c_3}^2\end{aligned} \tag{36b}$$

where $\bar{\lambda}(\mathrm{j}\omega)$ and $\tilde{\lambda}(\mathrm{j}\omega)$ are dependent on the system input and linear characteristic parameters k_1, c_1.

Consider further the specific situation where $u(t)=5\cos(\omega_0 t)$, $\omega_0=100$ rad/s, $k_1=10^4$ N/m and $c_1=30$ N/ms^{-1}.

For the purpose of evaluating the OFRF coefficients, take the constant vector $\boldsymbol{L}$ as

$$\boldsymbol{L}=\left[1, l_k, l_c, {l_k}^2, l_kl_c, {l_c}^2\right] \tag{37}$$

with $l_k=10^8, l_c=10^2$, and evaluate, by numerical simulations (Runge-Kutta method), the system output frequency responses under the following four selections of the design parameters.

$$k_3/l_k=\{0.01, 0.5, 2, 8\} \text{ and } c_3/l_c=\{0.01, 4, 10, 15\} \tag{38}$$

In this case, $\tilde{\boldsymbol{P}}_{\bar{N}\times\bar{M}}$ and $\tilde{\boldsymbol{\Lambda}}_{\bar{M}\times 1}$ with $\bar{M}=6$ and $\bar{N}=16$ in (28) and (26) are as follows,

$$\tilde{\boldsymbol{P}}_{16\times 6}=\begin{bmatrix}1 & (k_3/l_k)_{(1)} & (c_3/l_c)_{(1)} & (k_3/l_k)^2_{(1)} & (k_3c_3/l_kl_c)_{(1)} & (c_3/l_c)^2_{(1)}\\ \vdots & \vdots & \vdots & \vdots & \vdots & \vdots\\ 1 & (k_3/l_k)_{(16)} & (c_3/l_c)_{(16)} & (k_3/l_k)^2_{(16)} & (k_3c_3/l_kl_c)_{(16)} & (c_3/l_c)^2_{(16)}\end{bmatrix} \tag{39a}$$

$$\begin{aligned}\tilde{\boldsymbol{\Lambda}}_{6\times 1}=&\left[\lambda_{0,0}(\mathrm{j}\omega_0)\ \ l_k\lambda_{(1,0)}(\mathrm{j}\omega_0)\ \ l_c\lambda_{(0,1)}(\mathrm{j}\omega_0)\right.\\&\left.{l_k}^2\lambda_{(2,0)}(\mathrm{j}\omega_0)\ \ l_kl_c\lambda_{(1,1)}(\mathrm{j}\omega_0)\ \ {l_c}^2\lambda_{(0,2)}(\mathrm{j}\omega_0)\right]^{\mathrm{T}}\end{aligned} \tag{39b}$$

It is worth pointing out that there is no significant numerical difference among the components in matrix $\tilde{\boldsymbol{P}}_{16\times 6}$ thanks to the introduction of $\boldsymbol{L}$ in (37). This produces the OFRF coefficients

$$\tilde{\boldsymbol{\Lambda}}_{6\times 1}=\left(\tilde{\boldsymbol{P}}_{16\times 6}{}^{\mathrm{T}}\tilde{\boldsymbol{P}}_{16\times 6}\right)^{-1}\tilde{\boldsymbol{P}}_{16\times 6}{}^{\mathrm{T}}\bar{\boldsymbol{X}}_{16\times 1} \tag{40}$$

and, consequently, a theoretically equivalent but numerically more reliable OFRF representation for system (34) as follows.

$$\begin{aligned}Y(\mathrm{j}\omega_0)=&\left(0.120\times10^{-2}-0.636\times10^{-3}\mathrm{i}\right)+\\&\left(0.210\times10^{-4}+0.676\times10^{-4}\mathrm{i}\right)l_k{}^{-1}k_3+\\&\left(-0.499\times10^{-4}+0.137\times10^{-4}\mathrm{i}\right)l_c{}^{-1}c_3+\\&\left(-0.177\times10^{-5}-0.598\times10^{-6}\mathrm{i}\right)l_k{}^{-2}k_3{}^2+\\&\left(0.183\times10^{-6}-0.331\times10^{-5}\mathrm{i}\right)\left(l_kl_c\right)^{-1}k_3c_3+\\&\left(0.157\times10^{-5}-0.659\times10^{-7}\mathrm{i}\right)l_c{}^{-2}c_3{}^2\end{aligned} \tag{41a}$$

$$\begin{aligned}F_{out}(\mathrm{j}\omega_0)=&\left(13.978-2.771\mathrm{i}\right)+\left(0.211+0.676\mathrm{i}\right)l_k{}^{-1}k_3+\\&\left(-0.499+0.137\mathrm{i}\right)l_c{}^{-1}c_3+\\&\left(-0.018-0.591\times10^{-2}\mathrm{i}\right)l_k{}^{-2}k_3{}^2+\\&\left(0.178\times10^{-2}-0.033\mathrm{i}\right)\left(l_kl_c\right)^{-1}k_3c_3+\\&\left(0.016-0.668\times10^{-3}\mathrm{i}\right)l_c{}^{-2}c_3{}^2\end{aligned} \tag{41b}$$

Fig.2 shows the frequency spectra $|Y(\mathrm{j}\omega_0)|$ and $|F_{out}(\mathrm{j}\omega_0)|$ of system (34) with respect to the variation of $c_3\in[1, 15\times10^2]$ N/m^{3}s^{-3} in the case of $k_3=3\times10^8$ N/m^3. The results are determined by the OFRFs (41) and the numerical simulation, respectively. A comparison of these results clearly indicates a very good match between the OFRF representation and the accurate (simulated) result, demonstrating the effectiveness of the proposed OFRF determination method.

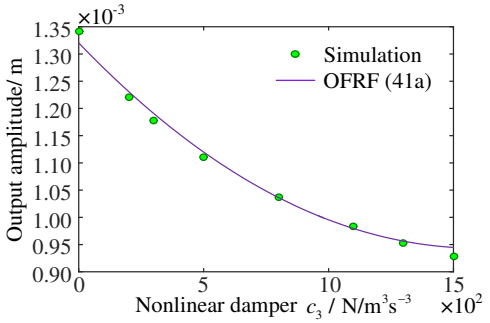

(a) Output spectrum of $Y(\mathrm{j}\omega_0)$

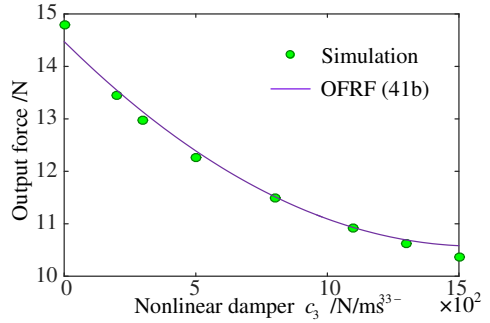

(b) Output spectrum of $F_{out}(\mathrm{j}\omega_0)$

Fig.2 A comparison of the output spectra of system (34) determined using the OFRF (41) with the numerical simulation results

In order to demonstrate how to follow the five step procedure in Section III-D to carry out a design, consider the design of the simple nonlinear system (33). The design objective is to achieve a specified force $f_{out}(t)$ for the system.

In this case, Steps 1 and 2 have been completed as the NARX-M-for-D (34) of the system has been established.

In Step 3, by designing the natural frequency of the system at $\omega_r = 100$ rad/s and the linear damping coefficient as $c_1 = 30$ N/ms, two design constraints in this case can be obtained as

$$\begin{cases} g_1(k_1, c_1, k_3, c_3): \sqrt{k_1} - 100 = 0 \\ g_2(k_1, c_1, k_3, c_3): c_1 - 30 = 0 \end{cases} \tag{42}$$

In Step 4, the OFRF representation of the spectrum of the output force of system (34) is obtained as given in (41b). By specifying $Y_0(\mathrm{j}\omega_0) = 12.0$ N, $\omega_0 = 100$ rad/s, and introducing two more constraints $k_3 \le 12\times10^8$ N/m^3 and $c_3 \le 15\times10^2$ N/m^{3}s^{-3} on the design parameters k_3 and c_3, the optimization problem (31) can now be formulized as:

Find

$$\boldsymbol{\xi}_0 = [k_1, c_1, k_3, c_3] \tag{43a}$$

to solve the optimization problem

$$\underset{\{k_1, c_1, k_3, c_3\}}{\mathrm{MIN}} \left| F_{out}(\mathrm{j}\omega_0) - 12.0 \right| \tag{43b}$$

under the constraint

$$\begin{cases} g_1(k_1, c_1, k_3, c_3): \sqrt{k_1} - 100 = 0 \\ g_2(k_1, c_1, k_3, c_3): c_1 - 30 = 0 \\ g_3(k_1, c_1, k_3, c_3): k_3 - 12\times10^8 \le 0 \\ g_4(k_1, c_1, k_3, c_3): c_3 - 15\times10^2 \le 0 \end{cases} \tag{43c}$$

The solution to the optimization problem (43) is straightforward. From the OFRF (41b), the relationship between $F_{out}(\mathrm{j}\omega_0)$ and the design parameters k_3 and c_3 can be obtained as shown in Fig.3 and 4.

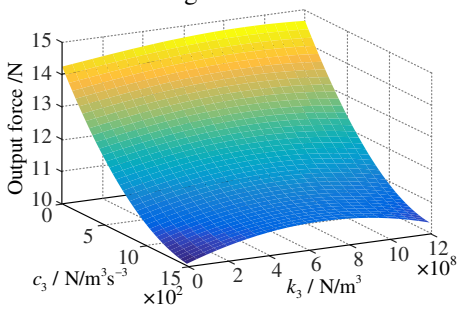

Fig.3 The output spectrum of system (33)

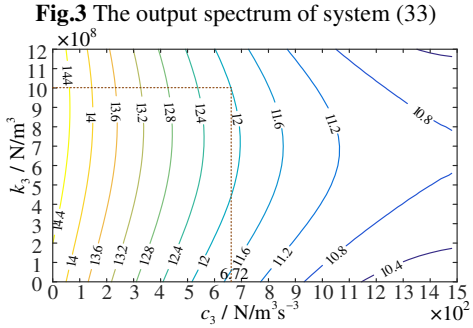

Fig.4 Contour map of the output spectrum of system (33)

According to Fig.4, the design for k_3 and c_3 can be reached simply by finding the values of k_3 and c_3 along the contour line of 12.0. For example, if selecting $k_3 = 10\times10^8$ N/m^3, along the contour line of 12.0 in Fig.4, k_3 can be obtained as $c_3 = 6.72\times10^2$ N/m^{3}s^{-3}. Consequently, a final design can be achieved as $k_1 = 10^4$ N/m, $c_1 = 30$ N/m^{3}s^{-3}, $k_3 = 10\times10^8$ N/m^3 and $c_3 = 6.72\times10^2$ N/m^{3}s^{-3}. Substituting the designed k_1, c_1, k_3 and c_3 into the system model (34) and, evaluating the output force of the system by simulation yields

$$F_{out}(\mathrm{j}\omega_0) = 12.241 \text{ N} \tag{44}$$

which is a good match to the design specification. Note that $k_3 = 10\times10^8$ N/m^3 is beyond the range of $k_3 = \{10^6, 0.5\times10^8, 2\times10^8, 8\times10^8\}$ N/m^3 over which the OFRF (41) was determined. This demonstrates that the OFRF is not a simple approximation but an inherent representation of the system output frequency response and can, therefore, be used to perform the system design over a wide range of the design parameter space.

In this case, the NARX-M-for-D of the system is established by discretizing an available physical differential equation model. However, in practice, a NARX-M-for-D often cannot be determined in this way as a differential equation model is often not available for complex physical systems. In next case study, a component of the system to design can only be described by a data-driven dynamic model. Consequently, the newly proposed NARX-M-for-D becomes a natural representation of the system that needs to be used to perform the system design.

B. Case study 2

In this case study, the design of the vibration isolation system shown in Fig.5 is considered where $M_0 = 1$ kg. $k_1 = \xi_1$ and $c_1 = \xi_2$ are the parameters of the spring and damper in the system. The isolator in the system is a piece of damping material which cannot be described by an analytical physical model but whose NARX-M-for-D has been determined under the sampling frequency $f_s = 512$ Hz as

$$f_{iso}(t) = a_1\xi_3 y(t) + a_2\xi_3 y^3(t) + a_3\xi_3 y^3(t-1) \tag{45}$$

by using nonlinear system identification techniques described in [28].

In (45), $f_{iso}(t)$ is the damping force produced by the isolator in the system, ξ_3 is the parameter of the isolator to be used for the system design, and

$$a_1 = 4\times10^{-3},\ a_2 = 10^4,\ a_3 = -0.75\times10^4 \tag{46}$$

are constants.

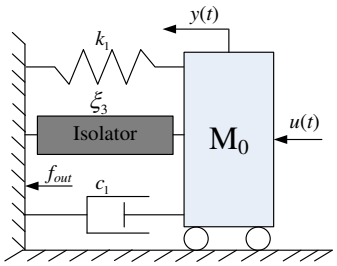

Fig.5 The vibration isolation system to design in Case study 2

According to the basic physical principle, the system in Fig.5 can be described as:

$$\begin{cases} u(t) = M_0\ddot{y}(t) + c_1\dot{y}(t) + k_1 y(t) + f_{iso}(t) \\ f_{out}(t) = c_1\dot{y}(t) + k_1 y(t) + f_{iso}(t) \end{cases} \tag{47}$$

From (45) to (47), the NARX-M-for-D of the isolation system can be obtained as:

$$\begin{cases}\bar{\theta}_{0,1}^{(1)}(\boldsymbol{\xi})u(t-1)+\bar{\theta}_{1,0}^{(2)}(\boldsymbol{\xi})y(t-2)+\bar{\theta}_{1,0}^{(1)}(\boldsymbol{\xi})y(t-1)+\\ \bar{\theta}_{3,0}^{(1,1,1)}(\boldsymbol{\xi})y^3(t-1)+\bar{\theta}_{3,0}^{(2,2,2)}(\boldsymbol{\xi})y^3(t-2)+\bar{\theta}_{1,0}^{(0)}(\boldsymbol{\xi})y(t)=0\\ \tilde{\theta}_{1,0}^{(1)}(\boldsymbol{\xi})y(t-1)+\tilde{\theta}_{1,0}^{(2)}(\boldsymbol{\xi})y(t-2)+\tilde{\theta}_{3,0}^{(1,1,1)}(\boldsymbol{\xi})y^3(t-1)+\\ \tilde{\theta}_{3,0}^{(2,2,2)}(\boldsymbol{\xi})y^3(t-2)-f_{out}(t-1)=0\end{cases} \tag{48}$$

which is clearly a specific case of the NARX-M-for-D (10) with $\boldsymbol{\xi}=[\xi_1,\xi_2,\xi_3]$, and the details of the coefficients are given in Appendix A.3.

In the following, the design of parameters $\boldsymbol{\xi}$ of the vibration isolation system when the system is subject to the multi-tone input

$$u(t)=6\cos(\omega_F t)+4\cos^3(\omega_F t) \tag{49}$$

where $\omega_F=100$ rad/s is considered. The design objective is to achieve a desired force transmissibility at the frequency ω_F as defined by

$$T(\mathrm{j}\omega)=\frac{F_{out}(\mathrm{j}\omega)}{U(\mathrm{j}\omega)} \tag{50}$$

where $U(\mathrm{j}\omega)$ and $F_{out}(\mathrm{j}\omega)$ is the spectrum of the input and output forces of the system, respectively.

From the NARX-M-for-D (48), the results in Steps 1 and 2 of the proposed general design approach are obtained, which are the NARX-M-for-D (48) and the relationship between the system design parameters $\boldsymbol{\xi}$ and the linear and nonlinear characteristic parameters of the system. In Step 3, three constraints on the design parameters $\boldsymbol{\xi}$ are introduced as

$$\begin{cases}g_1(\boldsymbol{\xi}):\xi_1-4\times10^{-3}\xi_3-10^4=0\\ g_2(\boldsymbol{\xi}):\xi_2-30=0\\ g_3(\boldsymbol{\xi}):\xi_1-6\times10^4\le0\end{cases} \tag{51}$$

to ensure that the FRF of the system at the driving frequency $\omega_F=100$ rad/s is as specified in the following

$$\begin{aligned}H_1(\mathrm{j}\omega_F)&=\frac{\bar{\theta}_{0,1}^{(1)}(\boldsymbol{\xi})\exp(-\mathrm{j}\omega_F\Delta t)}{1-\bar{\theta}_{1,0}^{(1)}(\boldsymbol{\xi})\exp(-\mathrm{j}\omega_F\Delta t)-\bar{\theta}_{1,0}^{(2)}(\boldsymbol{\xi})\exp(-2\mathrm{j}\omega_F\Delta t)}\\ &=3.469\times10^{-5}-3.320\times10^{-4}\mathrm{i}\end{aligned} \tag{52}$$

and $g_3(\boldsymbol{\xi})$ is a constraint on the maximum value of the stiffiness of the spring.

Moreover, in Step 4, the OFRF representation of the force transmissibility $T(\mathrm{j}\omega_F)$ of the system is determined. In this case, $N=11$

$$\tilde{\boldsymbol{\Xi}}=\bar{\boldsymbol{\Xi}}=\bigcup_{n=1}^{N}\bar{\boldsymbol{\Xi}}_n=\left[1,\xi_3,\xi_3^2,\xi_3^3,\xi_3^4,\xi_3^5\right] \tag{53}$$

and the OFRF was determined from the system output responses to input (49) when the design parameters ξ_3 changes over the range of $\{0.01, 0.8, 2, 3, 4, 5\}$ as

$$\begin{aligned}T(\mathrm{j}\omega_F)=&(-2.456+1.443\mathrm{i})+(1.383-4.098\mathrm{i})l_\xi^{-1}\xi_3+\\ &(-0.846+3.293\mathrm{i})l_\xi^{-2}\xi_3^2+(0.285-1.244\mathrm{i})l_\xi^{-3}\xi_3^3+\\ &(-0.047+0.220\mathrm{i})l_\xi^{-4}\xi_3^4+(0.306\times10^{-3}-0.015\mathrm{i})l_\xi^{-5}\xi_3^5\end{aligned} \tag{54}$$

where $l_\xi=10^6$

Based on the results of Steps 1-4 above, in Step 5, the design issue in this case study can be described as an optimal design probem as follows.

Find

$$\boldsymbol{\xi}_0=[\xi_1,\xi_2,\xi_3] \tag{55a}$$

to solve the optimization problem

$$\underset{\{\xi_1,\xi_2,\xi_3\}}{\mathrm{MIN}}\left|T(\mathrm{j}\omega_F)-1.5\right| \tag{55b}$$

under the constraint

$$\begin{cases}g_1(\boldsymbol{\xi}):\xi_1-4\times10^{-3}\xi_3-10^4=0\\ g_2(\boldsymbol{\xi}):\xi_2-30=0\\ g_3(\boldsymbol{\xi}):\xi_1-6\times10^4\le0\end{cases} \tag{55c}$$

where

$$\left|T(\mathrm{j}\omega_F)\right|=\sqrt{\mathrm{Re}^2\left[T(\mathrm{j}\omega_F)\right]+\mathrm{Im}^2\left[T(\mathrm{j}\omega_F)\right]} \tag{56}$$

and

$$\begin{cases}\mathrm{Re}\left[T(\mathrm{j}\omega_F)\right]=-2.456+1.383l_\xi^{-1}\xi_3-0.846l_\xi^{-2}\xi_3^2+\\ \qquad 0.285l_\xi^{-3}\xi_3^3-0.047l_\xi^{-4}\xi_3^4+0.306\times10^{-3}l_\xi^{-5}\xi_3^5\\ \mathrm{Im}\left[T(\mathrm{j}\omega_F)\right]=1.443-4.098l_\xi^{-1}\xi_3+3.293l_\xi^{-2}\xi_3^2-\\ \qquad 1.244l_\xi^{-3}\xi_3^3+0.220l_\xi^{-4}\xi_3^4-0.015l_\xi^{-5}\xi_3^5\end{cases} \tag{57}$$

Considering the constraints of $g_1(\boldsymbol{\xi})$ and $g_3(\boldsymbol{\xi})$, it can be obtained that

$$\xi_3=\frac{\xi_1-10^4}{4\times10^{-3}}\le12.5\times10^6 \tag{58}$$

Under the constraint of (58), inequality (55c) can be solved to yield

$$2.3\times10^6\le\xi_3\le12.5\times10^6 \tag{59}$$

Consequently, from (58) and (59), it can be obtained that

$$1.92\times10^4\le\xi_1\le6\times10^4 \tag{60}$$

Therefore, the feasible solutions to the design problem in the case study are:

$$\begin{cases}2.3\times10^6\le\xi_3\le12.5\times10^6\\ \xi_2=30\\ 1.92\times10^4\le\xi_1\le6\times10^4\end{cases} \tag{61}$$

If ξ_3 is designed as $\xi_3=2.3\times10^6$, the corresponding $\xi_1=k_1$ and $\xi_2=c_1$ can be obtained as $\xi_1=k_1=1.92\times10^4$ N/m, $\xi_2=c_1=30$ N/ms^{-1}. The time history of the output force and the corresponding transmissibility are shown in Fig.6, where a comparison with the result in the case of $\xi_1=k_1=1.92\times10^4$ N/m, $\xi_2=c_1=30$ N/ms^{-1} and $\xi_3=0$ can also be observed.

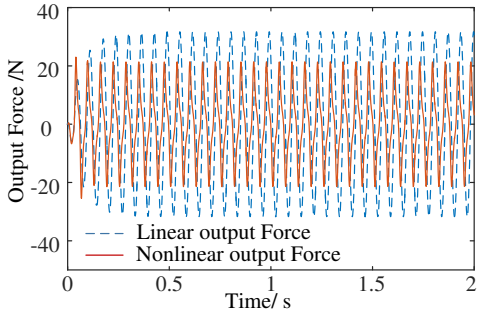

(a) Time history of the output force

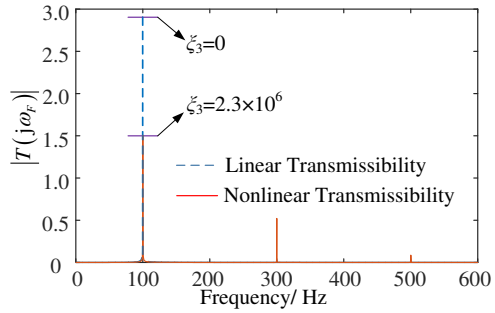

(b) The force transmissibility

Fig.6 A comparison of the system performances under the linear and nonlinear designs

From Fig.6, it can be observed that under the design, the transmissibility at the base frequency of $\omega_F = 100$ rad/s has reached 1.5 as required. But, compared to the case of $\xi_3 = 0$ where no material-based nonlinear isolator is introduced, the optimal design induces additional components at super harmonic frequencies, $\omega = 3\omega_F$ and $\omega = 5\omega_F$. However, the time history of the system response shown in Fig.6 (a) indicates that the optimal design has an overall better performance in vibration isolation. In order to confirm this observation, the concept of power transmissibility $E(\omega_F)$ introduced in [32]

$$E(\omega_F) = \frac{\int_0^{T_0} |f_{out}(t)|^2 \,\mathrm{d}t}{\int_0^{T_0} |u(t)|^2 \,\mathrm{d}t} = \sum_{p=1}^{\infty} \left| T(\mathrm{j}\omega)\big|_{\omega = p\omega_F} \right|^2, \quad T_0 = \frac{2\pi}{\omega_F} \tag{62}$$

was used to evaluate the vibration isolation performance of the system in the two cases. The results are

$$E(\omega_F) = 8.457 \tag{63}$$

when no material-based isolator is used and

$$E(\omega_F) = 2.559 \tag{64}$$

when the isolator is applied. Clearly, the optimal nonlinear design has achieved an overall better performance than the linear solution.

It is worth pointing out that because the optimisation problem is formulated using the OFRF which is a polynomial function of the design parameters, the numerical costs associated with the new design are normally less than the costs associated with a completely numerical simulation based method. In the case study above, for example, the overall computation on a standard PC running MATLAB codes only took 30 sec to complete.

V. Conclusions

Traditional nonlinear system designs are basically based on the time domain response analysis, which is often difficult to reveal the relationship between the system performance and the parameters that can be used to perform the design. Motivated by the wide engineering applications of the FRF-based linear system frequency domain analysis and design, the OFRF concept was proposed in order to extend the effective linear system approach to the nonlinear case. However, the methods required to know a differential equation-based physical model of the system where the physical parameters that can be used for analysis and design are the coefficients in the model.

Considering that it is difficult even impossible to find a differential equation model for complex engineering systems and the need to extend the physical model-based system design approach to address more complicated complex system designs, a new model known as the NARX-M-for-D is first proposed in the present study. A NARX-M-for-D can be derived from a nonlinear differential equation model of a system but, more importantly, can also be determined from the system input output data through a nonlinear system identification process. Moreover, a new OFRF-based methodology is developed that can be applied to the design of nonlinear systems described by a NARX-M-for-D. The methodology consists of a five step procedure including novel algorithm and technique for determining the structure and evaluating the coefficients of the OFRF of a NARX-M-for-D and can be applied to design a general class of nonlinear systems in the frequency domain. Two case studies have been provided to demonstrate the significance of the new design methodology.

The paper is basically concerned with the introduction of the NARX-M-for-D of nonlinear systems and the design of a nonlinear system based on the OFRF of the system's NARX-M-for-D. The determination of the NARX-M-for-D from practical testing data has been demonstrated in our previous works, and the focus of the present study is therefore the evaluation of the OFRF and the OFRF based optimal system design which is relevant to real world nonlinear system design.

The new design method, for the first time, transforms a complicated dynamic loading oriented engineering design into a much simpler polynomial-based optimal design problem. The method, therefore, has potential to be applied to address challenges with the optimal design of complex engineering systems and structures which, so far, can only be deal with using numerical simulation and random search etc. sophisticated and time consuming procedures.

Appendix A.1 The coefficients of NARX-M-for-D (6)

The model coefficients can be written as

$$\begin{aligned}
&\theta_{0,1}^{(1)}(\boldsymbol{\xi}) = 0.381\times10^{-5};\ \theta_{1,0}^{(0)}(\boldsymbol{\xi}) = -1;\\
&\theta_{1,0}^{(1)}(\boldsymbol{\xi}) = -\left(0.195\times10^{-2}c_1 + 0.381\times10^{-5}k_1 - 2\right);\\
&\theta_{1,0}^{(2)}(\boldsymbol{\xi}) = -\left(1 - 0.195\times10^{-2}c_1\right);\\
&\theta_{3,0}^{(1,1,1)}(\boldsymbol{\xi}) = -\left(0.381\times10^{-5}k_3 + 0.512\times10^{3}c_3\right);\\
&\theta_{3,0}^{(1,1,2)}(\boldsymbol{\xi}) = 1.023\times10^{3}c_3;\ \theta_{3,0}^{(1,2,2)}(\boldsymbol{\xi}) = -1.023\times10^{3}c_3;\\
&\theta_{3,0}^{(2,2,2)}(\boldsymbol{\xi}) = 0.512\times10^{3}c_3;\ \text{else } \theta_{p,q}^{(k_1,k_2,\cdots,k_{p+q})}(\boldsymbol{\xi}) = 0
\end{aligned} \tag{A1}$$

Appendix A.2. The coefficients of NARX-M-for-D (34)

The model coefficients can be written as

$$\begin{aligned}
&\bar{\theta}_{0,1}^{(1)}(\boldsymbol{\xi}) = 0.381\times10^{-5};\ \bar{\theta}_{1,0}^{(0)}(\boldsymbol{\xi}) = -1;\\
&\bar{\theta}_{1,0}^{(1)}(\boldsymbol{\xi}) = -\left(0.195\times10^{-2}c_1 + 0.381\times10^{-5}k_1 - 2\right);\\
&\bar{\theta}_{1,0}^{(2)}(\boldsymbol{\xi}) = -\left(1 - 0.195\times10^{-2}c_1\right);\\
&\bar{\theta}_{3,0}^{(1,1,1)}(\boldsymbol{\xi}) = -\left(0.381\times10^{-5}k_3 + 0.512\times10^{3}c_3\right);\\
&\bar{\theta}_{3,0}^{(1,1,2)}(\boldsymbol{\xi}) = 1.023\times10^{3}c_3;\ \bar{\theta}_{3,0}^{(1,2,2)}(\boldsymbol{\xi}) = -1.023\times10^{3}c_3;\\
&\bar{\theta}_{3,0}^{(2,2,2)}(\boldsymbol{\xi}) = 0.512\times10^{3}c_3;\ \text{else } \bar{\theta}_{p,q}^{(k_1,k_2,\cdots,k_{p+q})}(\boldsymbol{\xi}) = 0
\end{aligned} \tag{A2}$$

and

$$\begin{aligned}&\tilde{\theta}_{1,0}^{(1)}(\boldsymbol{\xi})=0.512\times10^{3}c_1+k_1;\ \tilde{\theta}_{1,0}^{(2)}(\boldsymbol{\xi})=-0.512\times10^{3}c_1;\\&\tilde{\theta}_{3,0}^{(1,1,1)}(\boldsymbol{\xi})=k_3+0.745\times10^{-8}c_3;\ \tilde{\theta}_{3,0}^{(1,1,2)}(\boldsymbol{\xi})=-0.149\times10^{-7}c_3;\\&\tilde{\theta}_{3,0}^{(1,2,2)}(\boldsymbol{\xi})=0.149\times10^{-7}c_3;\ \tilde{\theta}_{3,0}^{(3,3,3)}(\boldsymbol{\xi})=-0.745\times10^{-8}c_3;\\&\text{else }\tilde{\theta}_{p,q}^{(k_1,k_2,\cdots,k_{p+q})}(\boldsymbol{\xi})=0\end{aligned}\tag{A3}$$

such that

$$\tilde{\theta}_{p,q}^{(k_1,\cdots,k_{p+q})}(\boldsymbol{\xi})=f_s{}^{2}\bar{\theta}_{p,q}^{(k_1,\cdots,k_{p+q})}(\boldsymbol{\xi})=2.621\times10^{5}\bar{\theta}_{p,q}^{(k_1,\cdots,k_{p+q})}(\boldsymbol{\xi})\tag{A4}$$

for $p+q\ge 2$, and the condition of Corollary 1 is satisfied.

Appendix A.3. The coefficients of NARX-M-for-D (48)

The model coefficients can be written as

$$\begin{aligned}&\bar{\theta}_{0,1}^{(1)}(\boldsymbol{\xi})=0.381\times10^{-5};\ \bar{\theta}_{1,0}^{(0)}(\boldsymbol{\xi})=-1;\\&\bar{\theta}_{1,0}^{(1)}(\boldsymbol{\xi})=2-0.195\times10^{-2}\xi_2-0.381\times10^{-5}\xi_1-0.153\times10^{-9}\xi_3;\\&\bar{\theta}_{1,0}^{(2)}(\boldsymbol{\xi})=0.195\times10^{-2}\xi_2-1;\ \bar{\theta}_{3,0}^{(1,1,1)}(\boldsymbol{\xi})=-0.038\xi_3;\\&\bar{\theta}_{3,0}^{(2,2,2)}(\boldsymbol{\xi})=0.029\xi_3;\ \text{else }\bar{\theta}_{p,q}^{(k_1,k_2,\cdots,k_{p+q})}(\boldsymbol{\xi})=0\end{aligned}\tag{A5}$$

and

$$\begin{aligned}&\tilde{\theta}_{1,0}^{(1)}(\boldsymbol{\xi})=0.512\times10^{3}\xi_2+\xi_1+4\times10^{-3}\xi_3;\\&\tilde{\theta}_{1,0}^{(2)}(\boldsymbol{\xi})=-0.512\times10^{3}\xi_2;\ \tilde{\theta}_{3,0}^{(1,1,1)}(\boldsymbol{\xi})=10^{4}\xi_3;\\&\tilde{\theta}_{3,0}^{(3,3,3)}(\boldsymbol{\xi})=0.75\times10^{4}\xi_3;\ \text{else }\tilde{\theta}_{p,q}^{(k_1,k_2,\cdots,k_{p+q})}(\boldsymbol{\xi})=0\end{aligned}\tag{A6}$$

Appendix B. Proof of Proposition 2

According to (11a) and (11b), it can be seen that given linear coefficients $\bar{\theta}_{0,1}^{(.)}(\boldsymbol{\xi})$, $\bar{\theta}_{1,0}^{(.)}(\boldsymbol{\xi})$, $\tilde{\theta}_{0,1}^{(.)}(\boldsymbol{\xi})$ and $\tilde{\theta}_{1,0}^{(.)}(\boldsymbol{\xi})$, the n th order GFRFs of the (10a) can be written as [16]:

$$\begin{aligned}H_n^{x}(\omega_1,\cdots,\omega_n)&=\sum_{(v_1,\cdots,v_{sN})\in\boldsymbol{V}}\bar{h}_{(\bar{v}_1,\cdots,\bar{v}_{sN})}\bar{\theta}_1^{v_1}\bar{\theta}_2^{v_2}\cdots\bar{\theta}_{sN}{}^{v_{sN}}\\&=\bar{\boldsymbol{\Theta}}_n\bar{\boldsymbol{h}}_n(\omega_1,\cdots,\omega_n)\end{aligned}\tag{B1}$$

where $\boldsymbol{V}$ represents a sN-dimensional nonnegative integer vectors which contains the exponents of $\bar{\theta}_1^{v_1}\bar{\theta}_2^{v_2}\cdots\bar{\theta}_{sN}{}^{v_{sN}}$ and $\bar{h}_{(\bar{v}_1,\cdots,\bar{v}_{sN})}$ are constants, $\bar{\theta}_1,\bar{\theta}_2,\ldots,\bar{\theta}_{sN}\in\left[\bar{\theta}_{p,q}^{(k_1,\cdots,k_n)}(\boldsymbol{\xi})\middle|\,p+q\ge2\right]$.

Substituting (13) into (B1), yields:

$$\begin{aligned}H_n^{x}(\omega_1,\cdots,\omega_n)&=\sum_{i=1}^{N'}\bar{h}_{n:i}(\omega_1,\cdots,\omega_n)\bar{\boldsymbol{\xi}}_{(n:i)}\bar{\boldsymbol{\beta}}_{(n:i)}\\&=\bar{\boldsymbol{\Xi}}_n\bar{\boldsymbol{H}}_n(\omega_1,\cdots,\omega_n)\end{aligned}\tag{B2}$$

where $\bar{h}_{n:i}(\omega_1,\cdots,\omega_n)$ are the i th element of $\bar{\boldsymbol{h}}_n(\omega_1,\cdots,\omega_n)$, $\bar{\boldsymbol{\Xi}}_n$ is composed of $\bar{\xi}_{(n:i)}$, $i=1,\ldots,N'$, and N' is the maximum dimension of vector $\bar{\boldsymbol{\Theta}}_n$.

Substituting (B2) into (11a), yields:

$$\begin{aligned}Y(\mathrm{j}\omega)&=\sum_{n=1}^{N}Y_n(\mathrm{j}\omega)\\&=\sum_{n=1}^{N}\frac{1}{\sqrt{n}(2\pi)^{n-1}}\int_{\omega_1+\cdots+\omega_n=\omega}\bar{\boldsymbol{\Xi}}_n\bar{\boldsymbol{H}}_n(\omega_1,\cdots,\omega_n)\prod_{i=1}^{n}U(\mathrm{j}\omega_i)\mathrm{d}\sigma_\omega\\&=\sum_{n=1}^{N}\bar{\boldsymbol{\Xi}}_n\boldsymbol{X}_n(\mathrm{j}\omega)\end{aligned}\tag{B3}$$

where

$$\boldsymbol{X}_n(\mathrm{j}\omega)=\frac{1}{\sqrt{n}(2\pi)^{n-1}}\int_{\omega_1+\cdots+\omega_n=\omega}\bar{\boldsymbol{H}}_n(\omega_1,\cdots,\omega_n)\prod_{i=1}^{n}U(\mathrm{j}\omega_i)\mathrm{d}\sigma_\omega\tag{B4}$$

Similarly, it can be obtained that

$$Y(\mathrm{j}\omega)=\sum_{n=1}^{N}\tilde{\boldsymbol{\Xi}}_n\boldsymbol{Y}_n(\mathrm{j}\omega)\tag{B5}$$

Therefore, Proposition 2 is proven.

Appendix C. Proof of Proposition 3

In (11a), the n th order GFRFs' coefficient vector $\bar{\boldsymbol{\Theta}}_n$ can be calculated by using the algorithm discussed in Peng et al [33]:

$$\begin{aligned}\bar{\boldsymbol{\Theta}}_n=&\left[\bigcup_{k_1,\ldots,k_n=1}^{K}\bar{\theta}_{0,n}^{(k_1,\cdots,k_n)}(\boldsymbol{\xi})\right]\cup\left[\bigcup_{q=1}^{n-1}\bigcup_{p=1}^{n-q}\bigcup_{k_1,\ldots,k_n=1}^{K}\left(\bar{\theta}_{p,q}^{(k_1,\cdots,k_{p+q})}(\boldsymbol{\xi})\otimes\boldsymbol{\Theta}_{n-q,p}\right)\right]\\&\cup\left[\bigcup_{p=2}^{n}\bigcup_{k_1,\ldots,k_n=1}^{K}\left(\bar{\theta}_{p,0}^{(k_1,\cdots,k_p)}(\boldsymbol{\xi})\otimes\boldsymbol{\Theta}_{n,p}\right)\right]\end{aligned}\tag{C1}$$

where $\boldsymbol{\Theta}_{n,p}=\bigcup_{i=1}^{n-p+1}\left(\bar{\boldsymbol{\Theta}}_i\otimes\boldsymbol{\Theta}_{n-i,p-1}\right)$ and $\boldsymbol{\Theta}_{n,1}=\bar{\boldsymbol{\Theta}}_n$.

Substituting (13) into (C1), $\bar{\boldsymbol{\Xi}}_2$ can be obtained satisfying Proposition 3. Moreover, by using the mathematical induction and assuming Proposition 3 holds for $\bar{\boldsymbol{\Xi}}_n$, it can be obtained that

$$\begin{aligned}\bar{\boldsymbol{\Xi}}_{n+1}=&\left[\bigcup_{k_1,\ldots,k_{n+1}=1}^{K}\bar{\xi}_{0,n+1}^{(k_1,\cdots,k_{n+1})}\right]\cup\left[\bigcup_{q=1}^{n}\bigcup_{p=1}^{n+1-q}\bigcup_{k_1,\ldots,k_{n+1}=1}^{K}\left(\bar{\xi}_{p,q}^{(k_1,\cdots,k_{p+q})}\otimes\boldsymbol{\Xi}_{n+1-q,p}\right)\right]\\&\cup\left[\bigcup_{p=2}^{n+1}\bigcup_{k_1,\ldots,k_{n+1}=1}^{K}\left(\bar{\xi}_{p,0}^{(k_1,\cdots,k_p)}\otimes\boldsymbol{\Xi}_{n+1,p}\right)\right]\end{aligned}\tag{C2}$$

where, according to (11a), $\boldsymbol{\Xi}_{n+1,p}$ can be obtained as:

$$\begin{cases}\boldsymbol{\Xi}_{n+1,p}=\bigcup_{i=1}^{n+1-p+1}\left(\bar{\boldsymbol{\Xi}}_i\otimes\boldsymbol{\Xi}_{n+1-i,p-1}\right)\\\boldsymbol{\Xi}_{n+1,1}=\bar{\boldsymbol{\Xi}}_{n+1}\end{cases}\tag{C3}$$

Therefore, (16a) in the Proposition 3 is proven. For (16b), it can be proved by using the same process as from (C1) to (C3).

Appendix D. Proof of Corollary 1

From the condition $\tilde{\theta}_{p,q}^{(k_1,\cdots,k_{p+q})}(\boldsymbol{\xi})=\alpha\bar{\theta}_{p,q}^{(k_1,\cdots,k_{p+q})}(\boldsymbol{\xi})$ and (13), it is known that

$$\begin{aligned}\alpha\bar{\boldsymbol{\xi}}_{p,q}^{(k_1,\cdots,k_{p+q})}\bar{\boldsymbol{\beta}}_{p,q}^{(k_1,\cdots,k_{p+q})}&=\alpha\bar{\theta}_{p,q}^{(k_1,\cdots,k_{p+q})}(\boldsymbol{\xi})\\&=\tilde{\theta}_{p,q}^{(k_1,\cdots,k_{p+q})}(\boldsymbol{\xi})=\tilde{\boldsymbol{\xi}}_{p,q}^{(k_1,\cdots,k_{p+q})}\tilde{\boldsymbol{\beta}}_{p,q}^{(k_1,\cdots,k_{p+q})}\end{aligned}\tag{D1}$$

As $\bar{\boldsymbol{\xi}}_{p,q}^{(k_1,\cdots,k_{p+q})}$ and $\tilde{\boldsymbol{\xi}}_{p,q}^{(k_1,\cdots,k_{p+q})}$ are variables, (D1) indicates that

$$\begin{cases}\tilde{\boldsymbol{\beta}}_{p,q}^{(k_1,\cdots,k_{p+q})}=\alpha\bar{\boldsymbol{\beta}}_{p,q}^{(k_1,\cdots,k_{p+q})}\\\tilde{\boldsymbol{\xi}}_{p,q}^{(k_1,\cdots,k_{p+q})}=\bar{\boldsymbol{\xi}}_{p,q}^{(k_1,\cdots,k_{p+q})}\end{cases}\tag{D2}$$

and (16b) can be reduced to (16a) as

$$\begin{aligned}\tilde{\boldsymbol{\Xi}}_n=&\left[\bigcup_{k_1,\ldots,k_n=1}^{K}\bar{\xi}_{0,n}^{(k_1,\cdots,k_n)}\right]\cup\left[\bigcup_{q=1}^{n-1}\bigcup_{p=1}^{n-q}\bigcup_{k_1,\ldots,k_n=1}^{K}\left(\bar{\xi}_{p,q}^{(k_1,\cdots,k_{p+q})}\otimes\boldsymbol{\Xi}_{n-q,p}\right)\right]\\&\cup\left[\bigcup_{p=2}^{n}\bigcup_{k_1,\ldots,k_n=1}^{K}\left(\bar{\xi}_{p,0}^{(k_1,\cdots,k_p)}\otimes\boldsymbol{\Xi}_{n,p}\right)\right]=\bar{\boldsymbol{\Xi}}_n\end{aligned}\tag{D3}$$

Then Corollary 1 is proven.

REFERENCES

[1] V. Venkataramanan, K. Peng, B. M. Chen, and T. H. Lee, "Discrete-time composite nonlinear feedback control with an application in design of a hard disk drive servo system." *IEEE Trans. Control Syst. Technol.*, vol. 11,

no. 1, pp. 16-23, 2003.
[2] G. V. Kaigala, J. Jiang, C. J. Backhouse, and H. J. Marquez, "System design and modeling of a time-varying, nonlinear temperature controller for microfluidics." *IEEE Trans. Control Syst. Technol.*, vol. 18, no. 2, pp. 521-530, 2010.
[3] S. Glavaski, D.Subramanian, K. Ariyur, R. Ghosh, N. Lamba, and A. Papachristodoulou, "A nonlinear hybrid life support system: dynamic modeling, control design, and safety verification." *IEEE Trans. Control Syst. Technol.*, vol. 15, no. 6, pp. 1003-1017, 2007.
[4] A. Pavlov, N. Wouw, and H. Nijmeijer, "Frequency response functions for nonlinear convergent systems," *IEEE Trans. Autom. Control,* vol. 52, no. 6, pp. 1159-1165, 2007.
[5] L. Garbuio, M. Lallart, D. Guyomar, C. Richard, and D. Audigier, "Mechanical energy harvester with ultralow threshold rectification based on sshi nonlinear technique," *IEEE Trans. Ind. Electron.,* vol. 56, pp. 1048-1056, 2009.
[6] X. Jing, "Nonlinear characteristic output spectrum for nonlinear analysis and design," *IEEE-ASME Trans. Mechatron.,* vol. 19, no. 1, pp. 171-183, 2014.
[7] M. Alma, J. J. Martinez, I. D. Landau, and G. Buche, "Design and tuning of reduced order h-infinity feedforward compensators for active vibration control." *IEEE Trans. Control Syst. Technol.*, vol. 20, no. 2, pp. 554-561, 2012.
[8] M. Moradi, and A. Fekih, "A Stability Guaranteed Robust Fault Tolerant Control Design for Vehicle Suspension Systems Subject to Actuator Faults and Disturbances." *IEEE Trans. Control Syst. Technol.*, vol. 23, no. 3, pp. 1164-1171, 2015.
[9] M. H. Yao, Y. P. Chen, and W. Zhang, "Nonlinear vibrations of blade with varying rotating speed," *Nonlinear Dyn.*, vol. 68, no. 4, pp. 487-504, 2012.
[10] R. K. Pearson, *Discrete-time dynamic models*. Oxford University Press, 1999.
[11] K. Worden, and G. R. Tomlinson, *Nonlinearity in structural dynamics: detection, identification and modelling*. CRC Press, 2000.
[12] L. Liu, J. P. Thomas, E. H. Dowell, P. Attar, and K. C. Hall, "A comparison of classical and high dimensional harmonic balance approaches for a Duffing oscillator," *J. Comput. Phys.*, vol.215, no. 1, pp. 298-320, 2006.
[13] Z. K. Peng, Z. Q. Lang, S. A. Billings, and G. R. Tomlinson, "Comparisons between harmonic balance and nonlinear output frequency response function in nonlinear system analysis," *J. Sound Vib.*, vol.321, no. 1, pp. 56-73, 2008.
[14] D. A. George, *Continuous nonlinear systems*. Technical Report 335, MIT Research Laboratory of Electronics, 1959.
[15] Z. Q. Lang, and S. A. Billings, "Energy transfer properties of non-linear systems in the frequency domain," *Int. J. Control*, vol. 78, no. 5, pp. 345-362, 2005.
[16] Z. Q. Lang, S. A. Billings, R. Yue, and J. Li, "Output frequency response function of nonlinear Volterra systems," *Automatica*, vol.43, no. 5, pp. 805-816, 2007.
[17] P. Nuij, O. H. Bosgra, and M. Steinbuch, "Higher-order sinusoidal input describing functions for the analysis of non-linear systems with harmonic responses," *Mech. Syst. Signal Proc.*, vol. 20, no. 8, pp. 1883-1904, 2006.
[18] P. F. Guo, Z. Q. Lang, and Z. K. Peng, "Analysis and design of the force and displacement transmissibility of nonlinear viscous damper based vibration isolation systems," *Nonlinear Dyn.*, vol. 67, no. 4, pp. 2671-2687, 2012.
[19] X. J. Jing, Z. Q. Lang, S. A. Billings, and G. R. Tomlinson, "The parametric characteristic of frequency response functions for nonlinear systems," *Int. J. Control*, vol. 79, no. 12, pp. 1552-1564, 2006.
[20] D. Rijlaarsdam, T. Oomen, P. Nuij, J. Schoukens, and M. Steinbuch, "Uniquely connecting frequency domain representations of given order polynomial Wiener–Hammerstein systems," *Automatica*, vol. 48, no. 9, pp. 2381-2384, 2012.
[21] Z. K. Peng, and Z. Q. Lang, "The effects of nonlinearity on the output frequency response of a passive engine mount," *J. Sound Vib.*, vol. 318, pp. 313-328, 2008
[22] Z. Q. Lang, X. J. Jing, S. A. Billings, G. R. Tomlinson, and Z. K. Peng, "Theoretical study of the effects of nonlinear viscous damping on vibration isolation of sdof systems," *J. Sound Vib.*, vol. 323, no. 1, pp. 352-365, 2009.
[23] Z. K. Peng, Z. Q. Lang, L. Zhao, S. A Billings, G. R. Tomlinson, and P. F. Guo, "The force transmissibility of MDOF structures with a non-linear viscous damping device," *Int. J. Non-Linear Mech.*, vol. 46, no. 10, pp. 1305-1314, 2011.
[24] Q. Lv, and Z. Yao, "Analysis of the effects of nonlinear viscous damping on vibration isolator," *Nonlinear Dyn.*, vol. 79, no. 4, pp. 2325-2332, 2015.
[25] J. Schrock, T. Meurer, and A. Kugi, "Motion planning for piezo-actuated flexible structures: Modeling, design, and experiment." *IEEE Trans. Control Syst. Technol.*, vol. 21, no. 3, pp. 807-819, 2013.
[26] M. P. Castanier, and C. Pierre, "Modeling and analysis of mistuned bladed disk vibration: current status and emerging directions," *J. Propul. Power*, vol. 22, no. 2, pp. 384-396, 2006.
[27] S. Chen, and S. A. Billings, "Representations of non-linear systems: the NARMAX model," *International Journal of Control*, vol. 49, no. 3, pp. 1013-1032, 1989.
[28] H. L. Wei, Z. Q. Lang, and S. A. Billings, "Constructing an overall dynamical model for a system with changing design parameter properties," *International Journal of Modelling, Identification and Control*, vol. 5, pp. 93-104, 2008.
[29] J. C. Peyton-Jones, and S. A. Billings, "Recursive algorithm for computing the frequency response of a class of non-linear difference equation models," *Int. J. Control*, vol. 50, pp. 1925-1940, 1989.
[30] L. A. Aguirre, M. V. Correa, and C. C. S. Cassini, "Nonlinearities in NARX polynomial models: representation and estimation." *IEE Proc.-Control Theory Appl.*, vol. 149, no. 4, pp. 343-348, 2002.
[31] X. J. Jing, Z. Q. Lang, and S. A. Billings, "Frequency domain analysis for nonlinear Volterra systems with a general non-linear output function," *Int. J. Control*, vol. 81, no. 2, pp. 235-251, 2008.
[32] C. Ho, Z. Q. Lang, and S. A. Billings, "Design of vibration isolators by exploiting the beneficial effects of stiffness and damping nonlinearities," *J. Sound Vib.*, vol. 333, no. 12, pp. 2489-2504, 2014.
[33] Z. K. Peng, Z. Q. Lang, S. A. Billings, and Y. Lu, "Analysis of bilinear oscillators under harmonic loading using nonlinear output frequency response functions," *Int. J. Mech. Sci.*, vol. 19, no. 11, pp. 1213-1225, 2007.

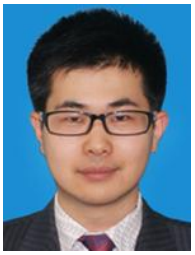

Yunpeng Zhu received the B.S. degree in Mechanical Engineering and Automation in 2013, and the M.S. degree in Mechanical Manufacturing and Automation in 2015, all from the Northeastern University, China. He is currently a Ph.D. student in the Department of Automatic Control and System Engineering, Sheffield University, UK. His research interests include analysis and design of nonlinear systems.

Z Q Lang received the B.S. and M.Sc. degrees in Automatic Control in China and the Ph.D. degree in Systems and Control Engineering from the Department of Automatic Control and Systems Engineering, University of Sheffield, U.K. He is currently the Chair Professor of Complex Systems Analysis and Design with the Department of Automatic Control and Systems Engineering, University of Sheffield. His main expertise relates to the theories and methods for complex systems modeling, analysis, design, signal processing, and the application of these to resolving various engineering problems, including smart structures and systems, civil and mechanical structure vibration control, structural health monitoring, and condition monitoring and fault diagnosis for wind turbine components and systems.